Australian Government
Department of Defence
Defence Science and
Technology Organisation

Effects of Dynamic Impact Loading on Microstructure of FCC (TWIP) Steel

C.H. Choi[1], *C.T. Peng*[2] *and B.F. Dixon*[1]

[1] **Land Division**
Defence Science and Technology Organisation

[2] Faculty of Engineering
University of Wollongong

DSTO-TR-3004

ABSTRACT

Armoured vehicles are primarily designed to provide protection against blast and ballistic events, however there is pressure to reduce the weight of vehicles in order to achieve improvements in range and maneouvrability combined with reductions in operating cost. To obtain improved performance without compromising blast and ballistic properties, a range of tougher, lighter and harder materials have been investigated. This work looks at the possible use of ultra-fine grain (UFG) materials to achieve the desired properties. From a fundamental viewpoint, as indicated by the Hall-Petch equation, UFG is an ideal means for hardening and strengthening a metal without changing its chemical composition and without compromising ductility.

The work described here is a microstructural investigation of TWIP steel that has been subjected to blast loading. It is found that the technique reduced the grain size of the TWIP steel significantly and that the dominant deformation mechanism of the grain refined material was dislocation slips. The reduction in grain size resulted in a considerable increase in material hardness

Published by

Land Division
DSTO Defence Science and Technology Organisation
506 Lorimer St
Fishermans Bend, Victoria 3207 Australia

Telephone: 1300 333 362
Fax: (03) 9626 7999

AR-016-045
August 2014

APPROVED FOR PUBLIC RELEASE

Effects of Dynamic Impact Loading on Microstructure of FCC (TWIP) Steel

Executive Summary

Armoured vehicles are primarily designed to provide protection against blast and ballistic events, however there is pressure to reduce the weight of vehicles in order to achieve improvements in range and manoevrability combined with reductions in operating cost. To obtain improved performance without compromising blast and ballistic properties, a range of tougher, lighter and harder materials have been investigated. This work looks at the possible use of ultra-fine grain (UFG) materials to achieve the desired properties.

As indicated by the Hall-Petch equation, grain refinement is one of the best means to strengthen a material without changing its chemical composition or sacrificing ductility. Fine grain materials are traditionally obtained by mechanical working with the use of techniques such as forging, cold rolling, deep drawing, etc. In this work, the potential for UFG production by explosive blasting is under investigation.

There are three reasons for wishing to look at Explosive loading; (a) Explosive working is conventionally used for the hardening of railway track and has proven to be highly effective, (b) Explosive loading has the potential to impart higher loads to the material than can be achieved by conventional techniques, and (c) Armoured vehicles are occasionally subjected to blast loading and it is important to know if this has a beneficial or detrimental effect on the armour material properties.

Preliminary work on the blast loading of candidate armour materials has suggested that blast loading can be effective at reducing microstructural grain size. Furthermore, anecdotal evidence is that armour materials that have been subjected to one blast show reduced deformation when subjected to a second (or subsequent) blast.

It is found that the pre-blast technique reduced the grain size of the TWinning Induced Plasticity (TWIP) steel significantly and that the dominant deformation mechanism of the grain refined material was dislocation slips. Hardness measurements also demonstrated that reduction in grain size was associated with a considerable increase in hardness.

The next phase of the work will look at measurement of the improved performance. The procedure to be trialled involves blast loading of armour plate prior to explosion bulge testing with the use of the DSTO modified trial procedure.

Authors

C. H. Choi
Land Division

Chang-Ho Choi obtained a Master's degree in Materials Science at Oregon State University and undertook PhD study at the University of Illinois and later at the University of New South Wales, where he received a PhD with a thesis on superconductors. He has been employed as a materials scientist at DSTO Maritime Platforms Division since 1998. During the period 1998 to 2006, he worked with the metallurgy section. From 2006 to 2009, he worked in the biology section and from 2009 onward, in the Armour Mechanics and Vehicle Survivability group at Maritime Division and later Land Division.

C.T. Peng
School of Mechanical, Materials & Mechatronic Engineering
University of Wollongong

Ching-Tun Peng received a Bachelor of Science in Electronics Engineering at the Chung Yuan Christian University (Taiwan) and obtained a Master of Science in Manufacturing Engineering at Bradley University (Illinois, USA). Since obtaining his Master's degree he has been employed as a research assistant engineer at Caterpillar Inc. (Illinois, USA) from 2005 to 2007. After a contract teaching job in Taiwan, he started his higher degree research and is currently pursuing a PhD degree at the University of Wollongong.

Brian F. Dixon
Land Division

Brian Dixon is a Principal Research Scientist in the Land Division of Defence Science and Technology Organisation. He has been employed at DSTO since 1978, undertaking experimental development and fundamental studies into weld metal solidification cracking in steels and stainless steels. He has also undertaken extensive work on improving the weld zone toughness of high strength steels. During 1989 and 1990 Brian worked at Kockums Laboratory in Sweden as part of DSTO's contribution to the submarine project. Since 2001, Brian has worked in a number of developmental positions, including Director, Program Office (Maritime), STCC for M1 and M6 and S&T Adviser for JP 2048.

Contents

1. INTRODUCTION 1

2. EXPERIMENTAL 2

3. RESULTS AND DISCUSSION 5
3.1 Hardness Test 5
3.2 SEM micrographs 5
3.3 EBSD microstructure characterisation 6
3.4 Texture analysis 10

4. CONCLUSIONS 11

5. ACKNOWLEDGEMENTS 11

6. REFERENCES 11

This page is intentionally blank

1. Introduction

There is an ongoing demand to develop new materials for motor vehicles with improved crash survivability and reduced weight/maintenance. It happens that materials for armour applications require similar energy absorbing properties when the major threat is from blast loading. The key requirement of an innovative material is, under severe deformation, the capability to absorb maximum energy without failing catastrophically. A concept of ultra-fine grain (UFG) was adopted in this current investigation. Generally, there are five different types of strengthening mechanisms for metals: solid solution hardening, precipitation hardening, dispersion hardening, work hardening and grain refinement hardening. The strengthening mechanisms applied for this study were work hardening by plastic deformation and grain refinement hardening by reducing grain size. Grain refinement is a technique for strengthening a material without changing its chemical composition and compromising ductility. UFG materials generally show some excellent properties such as ultrahigh strength, enhanced fatigue behaviour and superior corrosion resistance. If grain refinement strengthening is effective for auto-related applications it may be also suitable for armour applications, which require similar properties.

One efficient technique for producing UFG materials is severe plastic deformation (SPD). Several SPD processing techniques have been developed to obtain UFG structures in both bulk and sheet materials. These techniques include equal-channel angular pressing (ECAP) [1-3], high-pressure torsion (HPT) [4], multi-axial compression/forging (MAC/F) [5] and accumulative roll bonding (ARB) [6-7]. Most techniques for SPD use relatively static or quasi-static low strain rate techniques, whereas blast loading is a rapid straining technique and there is insufficient information concerning the effect of rapid/high impact loading on grain size and the consequent effect of this process on strength and ductility. Therefore it is worthwhile to study the effect on microstructure (especially on grain size) of materials subjected to blast loading.

Work hardening rate is an indicator for measuring the strength variation of a material. The Hollomon [8] law proposes the relationship between work hardening exponent and true stress, strain, as shown in equation 1, below:

$$\sigma = K\epsilon^n \qquad (1)$$

where σ is true stress, ε is true strain, K and n are work hardening coefficient and work hardening exponent, respectively. Equation (2) is obtained by modifying Equation (1):

$$ln\sigma = nln\varepsilon + lnK \quad (2)$$

It is clear from Equation (2) that n plays a dominant role over instantaneous hardening rate. The n (work hardening exponent) value depends on the atomic structure, for Face Centre Cubic (FCC) metals n <0.6, for Body Centre Cubic (BCC), n <0.2 and for Hexagonal Close Packed (HCP), n <0.0002. For this reason, it is desirable to select FCC structures to study the effects of UFG. Furthermore among FCC structures, the chosen material should have very high energy absorption ability. It happens that TWinning Induced Plasticity (TWIP) steel is

one of the best candidates for this work. This material also satisfies the requirements of toughness, ductility and corrosion resistance.

Dini *et al* [9] argued that the optimum mechanical properties of TWIP steel as a function of work hardening capacity can be obtained by reducing the grain size. They also argued that the mechanical twinning increases with increased applied strain and, as a result, the material also has a high instantaneous work hardening due to the mechanical twin boundaries increasing yield stress.

Peng *et al* [10] observed that if the grain size is between 20 and 40 μm the twinning effect is optimised while finer grain sizes suppress the TWIP effect. Li *et al* [11] also argued tensile strength increases with increasing strain rate. Other effects, however, such as thermal softening, microstructure refining and adiabatic shear bands (ABS) may appear when the steel is subjected to high strain rate deformation. They concluded the following:

1. For TWIP steel deformed under dynamic conditions, the stress, microhardness and work hardening rates increase with the increase of the strain and strain rate, however, there is a decline of the work hardening rate if adiabatic temperature softening occurs.
2. The grain size after dynamic deformation is bigger than before, which suggests that recrystallization has occurred.
3. The interaction of twins with dislocations and twins with twins, and emergence of multiple deformation twins are the main strengthening mechanisms of the TWIP steel.

In the current investigation, a plate of TWIP steel that has been subjected to standard Explosion Bulge (EB) testing is investigated to identify the effect of blast loading on material microstructure and hardness.

2. Experimental

Figure 1 shows the standard EB test setup in which the die block with the test plate located on top of it was placed beneath the suspended charge. The distance from the die block to the bottom of the charge was 320 mm. The plate had holes drilled into opposing corners to enable clamping with a bolted shackle in order to stop the blasted plates impacting the ceiling of the blast chamber. A TWIP steel plate (760 mm x 760 mm x 8.5 mm) was selected as a trial material in this case.

The Explosive Bulge Test (EBT) was performed on the TWIP steel using charge weight (PE4 high explosive) of 2.3 kg. The explosive charge was cylindrical and 160 mm in diameter.

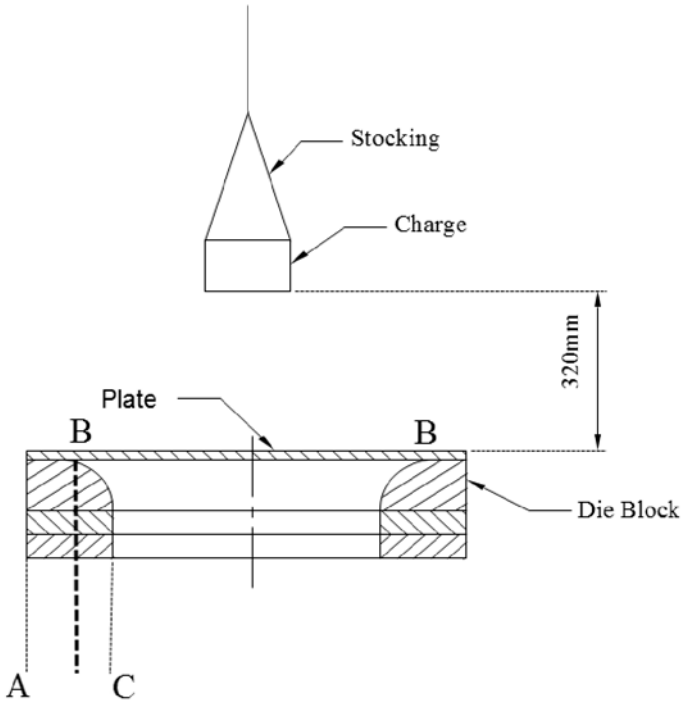

Figure 1:. Test configuration. The plate is held on top of an annular-shaped die block and the charge was suspended from the ceiling in a stocking. 'B-B' represents the touching annulus between a plate and the die block. The inside diameter of the annulus B-B is approximately 635 mm. The A-B and B-C distances are 140 mm and 89 mm, respectively.

In this investigation, the EBT was carried out at ambient temperature (≈17°C) and deformation resistance of the plate was measured in terms of bulge depth and plate thinning. The bulge depth of the plate was measured as a distance from the flat surface of the plate to the maximum bulge at the centre of the plate after a blast. Figure 2 shows the aluminium bulge depth measuring device in which the centre point has a small hole to be fitted with a digital depth ruler. Thinning of the plate was measured by ultrasonic thickness testing of the plate at its centre after testing and subtracting this figure from the thickness of the undeformed plate, as measured prior to blasting.

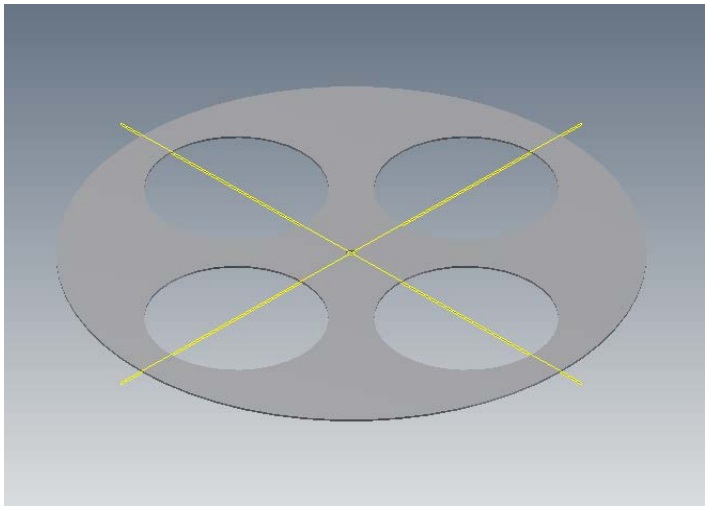

Figure 2: Aluminum bulge depth gauge

Table 1: Chemical composition of the TWIP steel with ultimate tensile strength of 940 MPa

.Composition (in mass %)						
Mn	Al	C	Cr	Si	Ni	Fe
17.85	1.31	0.592	0.368	0.223	0.101	Bal.

The chemical composition of the TWIP steel is shown in Table 1. The most notable feature of the steel is the high level of manganese (18%) combined with significant levels of aluminium, carbon, chromium and silicon.

Figure 3(a) shows a schematic diagram of the deformed TWIP steel plate. Six specimens with 10 x10 mm dimension were taken at 70 mm interval from the center of the plate. Micro and Macro-hardness testing was undertaken using a fully automatic hardness tester, Struers DuraScan-70, with a 0.5 kg and 10 kg load to determine the hardness effect with various specimens. It is notable in Figure 3(b) that the horizontal and transverse directions of the specimens were determined by the charge position. The microstructure was analyzed by both scanning electron microscope (SEM) and the electron back scattered diffraction (EBSD) technique which were conducted on a JEOL JSM-7001F field emission gun (FEG) fitted with a Nordlys–II(S) camera and the EBSD software, AZtecHKL at 15 kV, ~3.3nA and 24 mm working distance. The step size was 1 µm and the acquisition time was about 1.5 hour for a 300x230 µm² scanned area. Post processing of the obtained data was statistically analysed by HKL Channel-5 software.

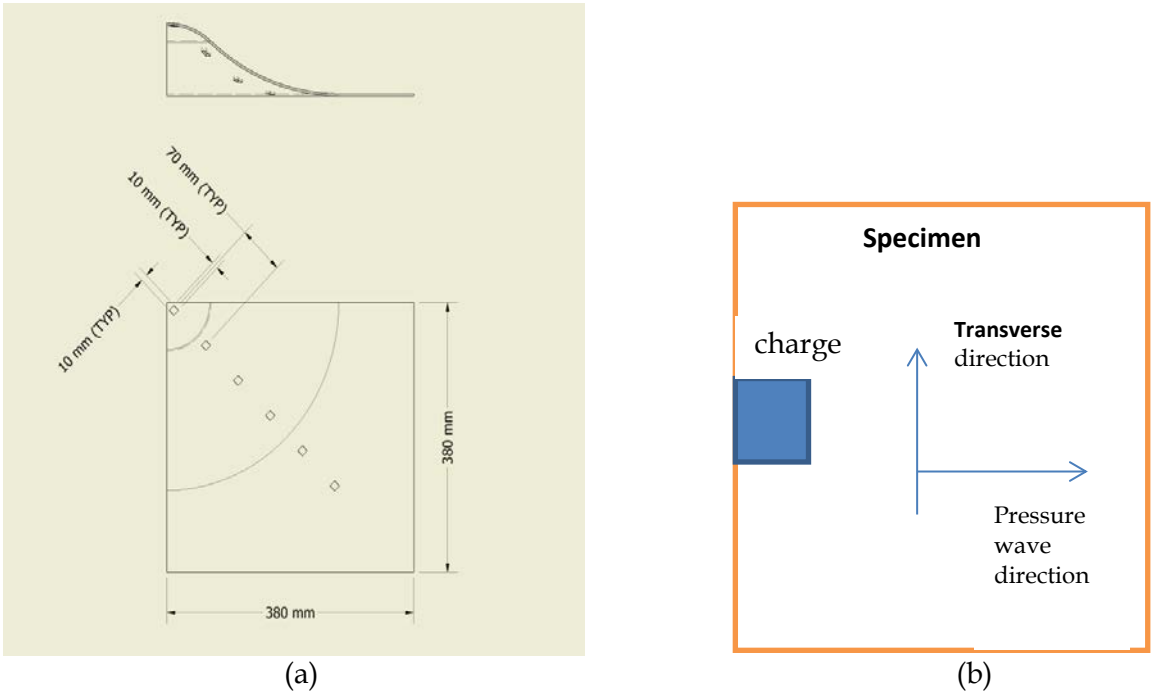

(a) (b)

Figure 3: a) Schematic diagram, showing one quarter of the bulged plate (upside down) and b) the transverse and the pressure wave direction determined by the position of the charge. The bulge depth of the deformed plate in this case was 166 mm.

3. Results and Discussion

3.1 Hardness Test

The micro- and macro-hardness test was performed with HV 0.5 and 10 kg loads, respectively. The values of hardness are presented in Figure 4. It is notable that, with two different loads of hardness tests, there is a tendency of declining value with the specimen away from the centre (specimen 1). The macro-hardness of specimen 6 shows almost identical value to the original hardness of the TWIP steel (230 HV) which implies that this area was not affected significantly by the impact. From micro-hardness test, specimen 5 showed an increase of the hardness. This was corresponded to 'C' position in Figure 1 where an additional impact would be added by the geographical constraint of the die block (between sample 4 and sample 5). This observation was well matched with the previous paper [12] when the specimen numbering system in increasing order was compared with the corresponding annealing temperatures in which higher annealing temperatures resulted in larger grain size.

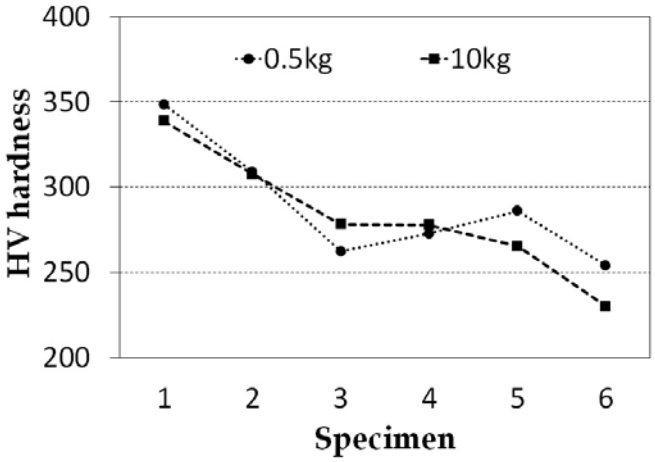

Figure 4: The hardness of TWIP specimens with a) 0.5 kg, and b) 10 kg HV loading (Specimen 1 is in the centre of the bulge with the greatest deformation).

3.2 SEM micrographs

Figure 5 shows the SEM images of 6 specimens. It is clear in the figure that with increase of specimen number, the grain size is increased. In another words, less damaged areas clearly have larger grain size.

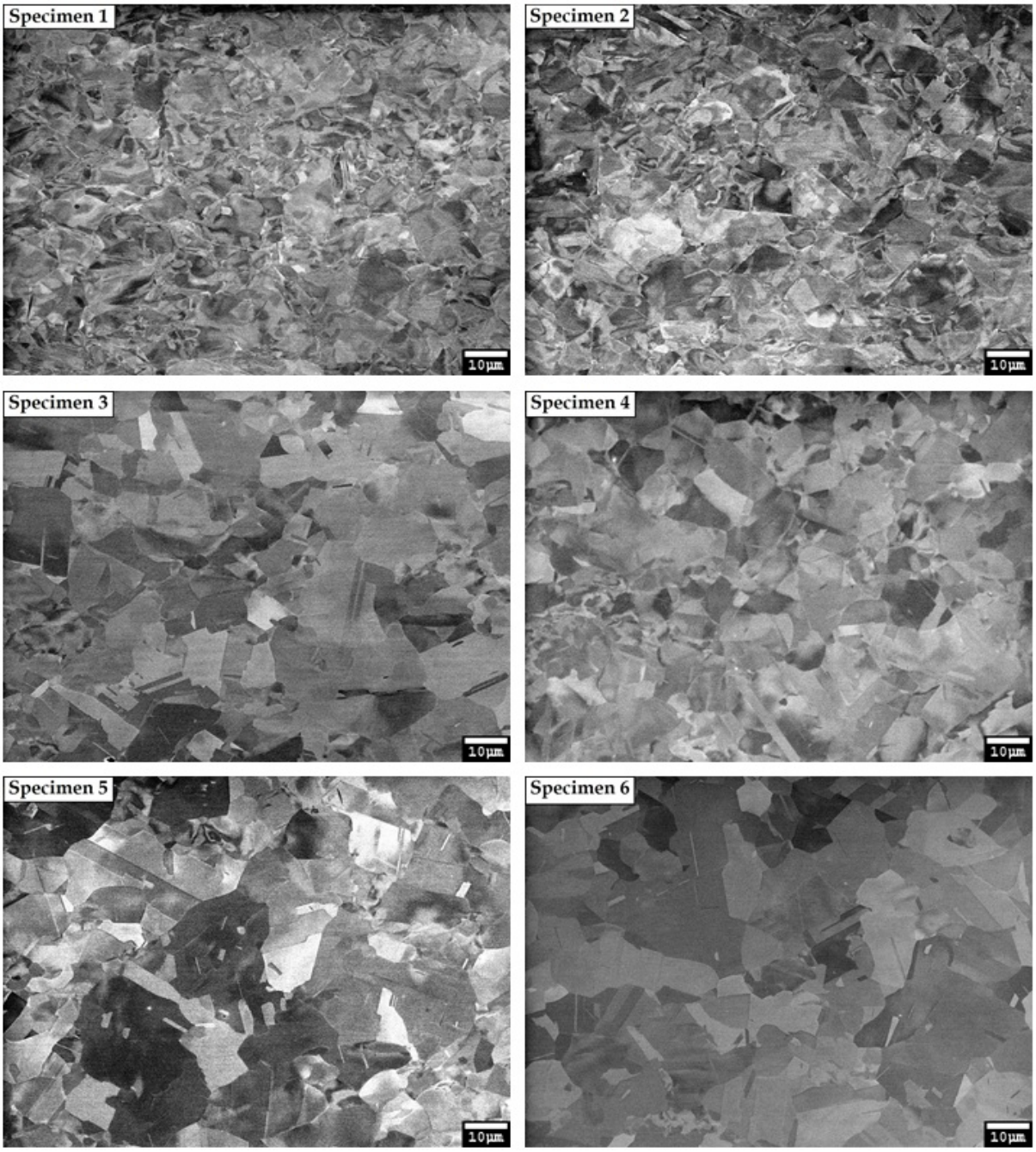

Figure 5: SEM images for the various blasted specimens

3.3 EBSD microstructure characterisation

EBSD grain boundary images of all the specimens are shown in Figure 6. The black lines indicate high angle grain boundaries (HAGBs) with critical misorientation > 15^0, the grey lines represents the low angle grain boundaries (LAGBs) with $2° \leq \theta < 15°$ (the misorientations less than 2° were disregarded). The total high angle grain boundaries (THAGBs) consists of HAGB and twin boundaries (TBs). First order twin boundaries (TBs) are defined as Σ3=60° <111>, shown in red lines, while second order TBs are Σ9=38.9° <101>, represented in blue lines, yielding tolerance limit of 6° for Σ3 and 2.4° for Σ9, respectively (following the Palumbo–Aust criterion) [12].

From the observation, specimen 1 has the finest grain size and there is a growing tendency of grain size from Specimen 1 to 6, which is in good agreement with the results of hardness tests. The first order TBs, Σ3 (red lines), are evenly distributed in all the samples. A small amount of second order TBs, Σ9 (blue lines) is also observed in those six maps. LAGBs were most predominant in Specimen 1 and 2.

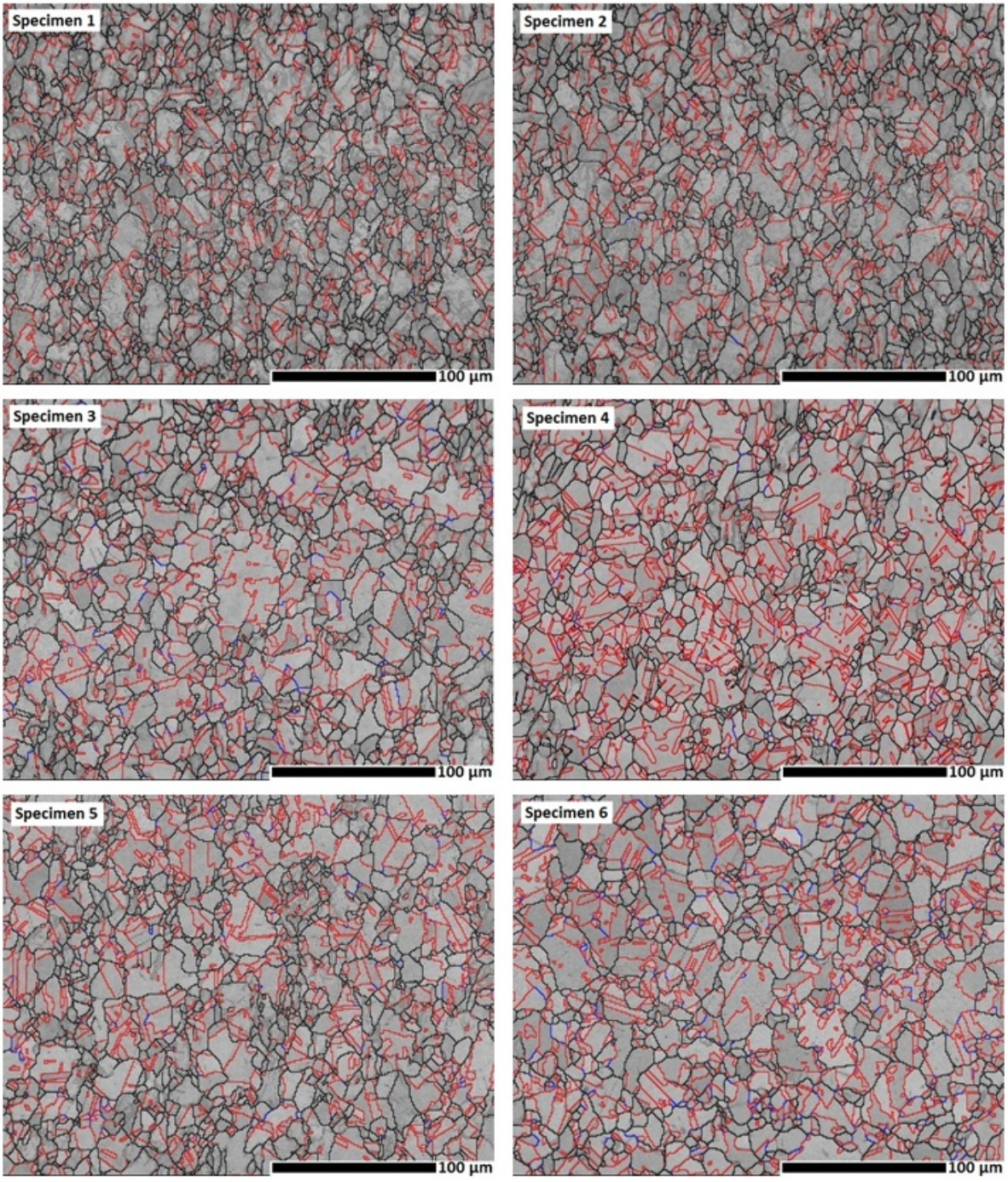

Figure 6: EBSD grain boundaries map for the specimens

Each map in Figure 6 is composed of scanned data points (pixel), moreover, the data can be statistically analysed to study the microstructure characters. Figure 7(a) shows the change in the misorientation distribution of the specimens at various locations, as cold rolled (As-CR,

original sample), and the curve of the theoretical random orientation. Two peaks were observed with representative misorientation axis distribution in the crystal coordinate system. The first order TBs or Σ3 resulted in the intense peak around 60° (related to <1 1 1>), on the other hand, the smaller peak at ~39°, <1 0 1>, represents the Σ9 or second order TBs. It is notable in the figure that first order twin (Σ3) boundary area at ~ 60° increases with increasing specimen number. At low misorientation angle, Specimen 1 and 2 revealed high relative frequency while at high misorientation angle, Specimen 5 and 6 were higher.

Figure 7(b) was extracted from the data of Figure 7(a). Σ3 boundary area fraction was calculated as the value of correlated frequency of 60° divided by the sum of the frequency. Same method was used to calculate Σ9, THAGBs, HAGBs and LAGBs area fraction. It is also evident in this figure that Σ3 and HAGBs increases with the increase of specimen number which is associated with a decrease in LAGBs and the evolution of Σ9 TBs. Secondary twins are relatively rare for the material in all conditions.

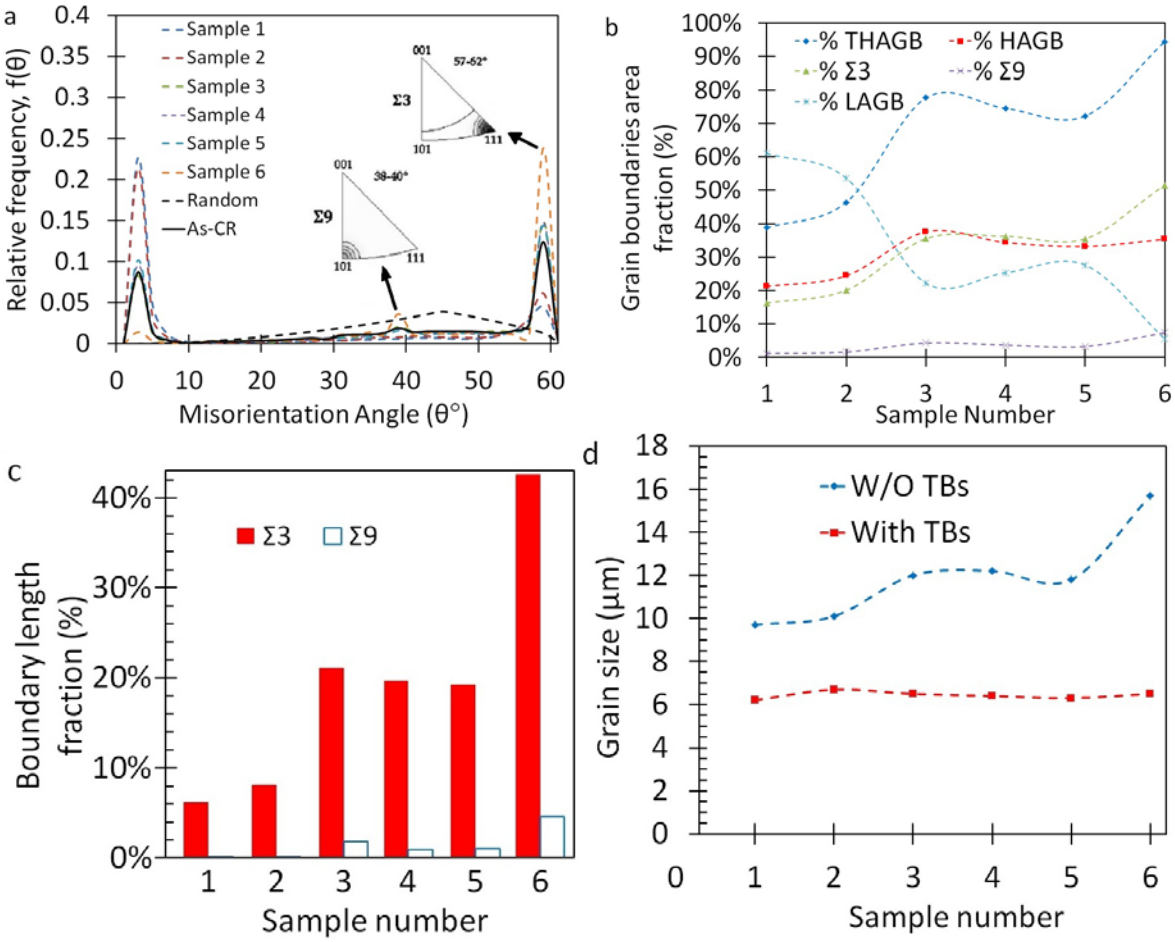

Figure 7: (a) Change in misorientation distribution as a function of various specimens with representative misorientation axis distributions in the crystal coordinate system for Σ3 and Σ9 angular ranges, (b) grain boundary area fraction as a function of various specimens, and (c) evolution of length fraction of Σ3 and Σ9 twin boundaries with various specimens. Σ3 = 60° <1 1 1> with 6° deviation, Σ9 = 38.9 <1 0 1> with 2.4° deviation and (d) change in grain size with and without taking TBs into account with various specimens.

The boundary with high Σ might be expected to have a higher energy than the one with low Σ. At low-angle boundaries, the distortion is entirely accommodated by dislocations, refer to Figure 7(a). For this reason it is concluded that the main strengthening mechanism is work hardening caused by grain refinement resulted from the high impact. However, the twin effects cannot be ignored because the dislocations created by the impact will cross over the twin boundaries. This result is clear in figure 7(c). The boundary length fraction increased with the increase of the specimen number. It implies that the existing TBs in more highly deformed regions were consumed by the interaction with dislocations created by the rapid deformation.

It is postulated that the first hardening mechanism is dominated by the dislocations created by the impact. The second hardening mechanism is due to the shorter dislocation mean free path cut by deformed twins which turns into more accumulated dislocation. This is in agreement with Kim et al [13].

Figure 7(d) reinforces this assumption. The figure shows the change in grain size with and without twin boundaries (TBs). When taking TBs into account, the twin boundaries (both Σ3 and Σ9) were behaving as grain boundaries, therefore, the average grain size is smaller compared with the grain size without taking TBs into account. The grain size without TBs increases with specimen number while the grain size with TBs is steady. The results indicate that the number of twin grain boundaries is evenly distributed over the specimen area, regardless of the original grain size. They also imply that twins may play an important role on this strengthening mechanism.

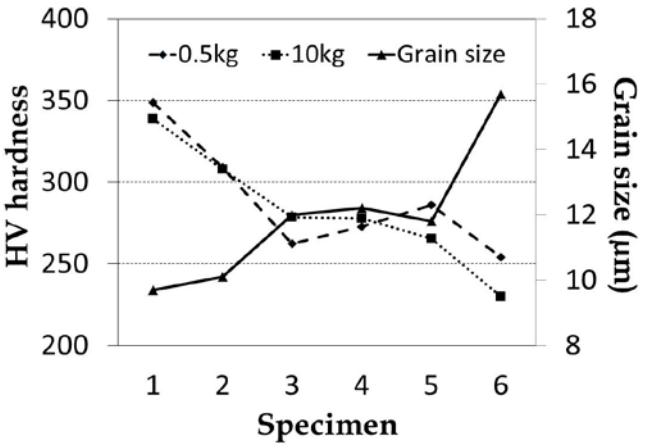

Figure 8: The relationship between hardness (both 0.5 kg and 10 kg) and grain size (without TBs) with various specimens.

It is denoted in this figure that the grain size (without TBs) has a trend to increase with the increase of the specimen number, i.e., reduction in deformation even though there was a complex pattern owing to the uneven deformation pattern of the specimens. This is contrary to the results of Le et al [11] in which the grain size after the deformation is larger than before. Figure 8 combined the results of figure 4 and 7(d). The hardness decreases with increasing sample number and the grain size increases with increasing sample number. Based on this result, therefore, it is concluded that the pre-impact loading method can be applied to any materials for higher strengthening.

3.4 Texture analysis

To study the development of crystallographic texture as a result of explosive loading, pole figures were derived from the collected results of EBSD data. In the form of stereographic projections, a pole figure is a two dimensional graphical representation of the orientation distribution of crystallographic lattice planes in the material. In this example, (1 1 1) pole figures were displayed representatively in the current investigation. Figure 9(a) shows the typical rolling texture components in FCC alloys [12] as reference, consisting of ideal orientation components, including Cube {1 0 0}<0 0 1>, Goss {1 1 0}<0 0 1>, Brass {1 1 0}<1 1 2>, Copper {1 1 2}<1 1 1>, and S {1 2 3}<6 3 4>.

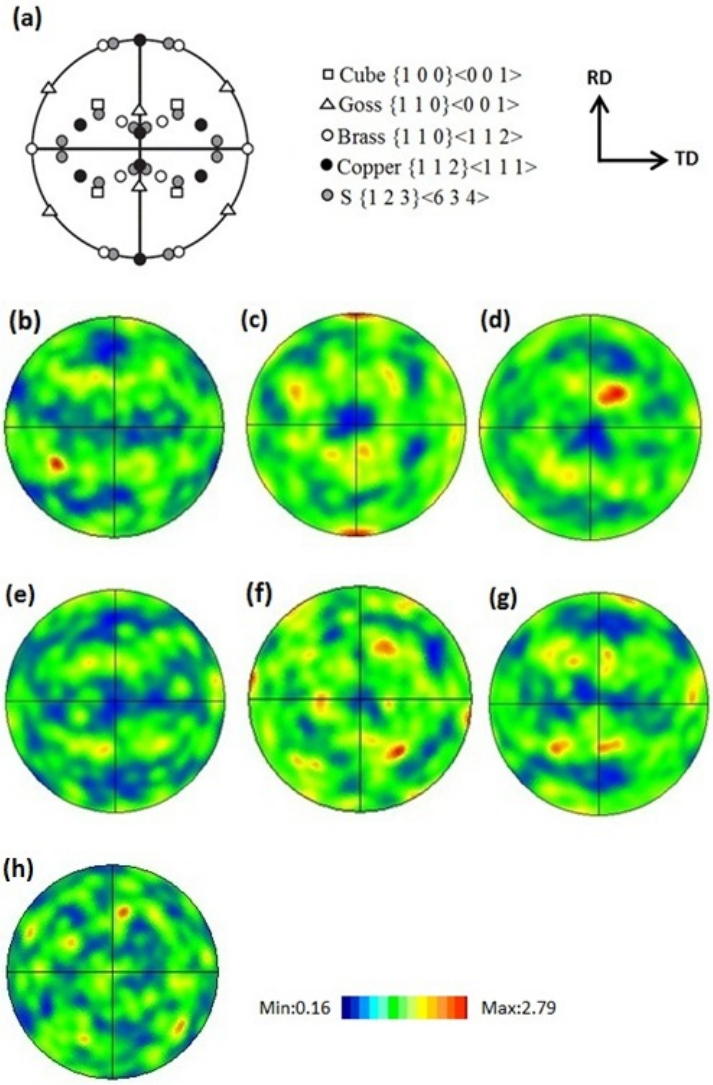

Figure 9: (1 1 1) pole figures of the (a) ideal rolling texture components in FCC materials, and (b) original, (c) Specimen 1, (d) Specimen 2, (e) Specimen 3, (f) Specimen 4, (g) Specimen 5, (h) Specimen 6.

From the experiments undertaken in this investigation, Figure 9(b) displays the (1 1 1) pole figure of the original Fe-18Mn-0.6C-1.5Al steel, while Figure 9(c-h) exhibit Specimen 1 to 6, respectively. It can be inferred that for the original specimen, the texture component was mainly cube type {0 0 1}<1 0 0> with minor copper type {1 1 2}<1 1 1> which possess greater

Schmid's factor of dislocation slip [9]. The pole figure of Specimen 2, 3 and 5 revealed the similar pattern of pole figure to the original (un-impacted) pattern. The pole figures of all other specimens did not show consistent patterns but random ones. This is due to the both the non-directional deformation and the huge energy released during blast experiments.

4. Conclusions

1. The main strengthening mechanism was the grain refinement created by the high impact.
2. Twin boundary development may be an alternative means of improving the strength of steel.
3. There may be signs of softening effect by annealing. It is crucial to optimise the charge weight to reduce the effects of recrystallization or annealing.
4. Cube type {001} <100> to brass type {110} <112> structures were predominant on the steel after blast loading. It is evident from this pattern that the twins occur heavily during deformation of this steel, while slip makes a contribution.
5. Sigma 9 (secondary twin) did not significantly affect the grain size in this work.

5. Acknowledgements

The authors acknowledge use of FEG-SEM JEOL–JSM7001F within the UOW Electron Microscopy Centre funded by the Australian Research Council.

6. References

1. Valiev, R. Z., Krasilnikov, N. A., Tsenev, N. K., 1991, Plastic deformation of alloys with submicro-grained structure, Mater. Sci. Eng. A137, 35-40.
2. Valiev, R. Z., Islamgaliev, R. K. and Alexandrov, I. V., 2000, Bulk nanostructured materials from severe plastic deformation, Progress in Materials Science 45, 103-189.
3. Valiev, R. Z. and Langdon, T. G., 2006, Principles of equal-channel angular pressing as a processing tool for grain refinement, Progress in Materials Science 51, 881-981.
4. Smirnova. N. A., Levit, V. I., Pilyugin, V. I., Kuznetsov, R. I., Davydova, L. S., Sazonova, V. A., 1986, Evolution of structure of f.c.c. single crystals during strong plastic deformation, Phys. Met. Metall., 61, No.6, 127-134.
5. Salishchev, G. A., Valiahmetov, O. R., Galeev, R. M.. 1993, Formation of submicrocrystalline structure in titanium alloy VT8 and its influence on mechanical properties, J. Mater. Sci., 28, 2898-2902.
6. Saito, Y., Tsuji, N., Utsunomiya, H., Sakai, T. and Hong, R.G., 1998, Ultra-fine grained bulk aluminum produced by accumulative roll-bonding (ARB) process, Scripta Materialia 39, 1221-1227
7. Saito, Y., Utsunomiya, H., Tsuji, N. and Sakai, T., 1999, Novel ultra-high straining

process for bulk materials development of the accumulative roll-bonding (ARB) process, Acta Materialia 47, 579-583.
8. Hollomon. J, 1945, Tensile deformation, Trans, Metall.Soc, 162, 268-290
9. G. Dini, A. Najafizadeh, R. Ueji, S.M. Morir-Vaghefi, 2010, Tensile deformation behavior of high manganese austenitic steel: The role of grain size, Materials and Design 31, 3395-3402.
10. C. Peng, M. Callaghan, H. Lee, K. Yan, K. Liss, T. Ngo, P. Mendis, C. Choi, 2013, On the compression behavior of an Austenitic Fe-18Mn-0.6C-1.5Al Twinning Induced Plasticity Steel, Steel Research International, 84, no 9999 1-7.
11. L. Zhao, W. Hui, L. Yue, H. Feng, L. Feng, J. Zhe, 2010, Effects of high strain rate on properties and microstructure evolution of TWIP steel subjected to impact loading, J of Iron and Steel Research, 17 (6), 67-73.
12. A.A. Saleh, E.V. Pereloma, A.A. Gazder, 2011, Texture evolution of cold rolled and annealed Fe-24 Mn-3 Al-2Si-1Ni-0.06C TWIP steel, Mater Sci. Eng. A, 528, 4537-4549.
13. J.K. Kim, L. Chen, H.S. Kim, S.K. Kim, G.S. Kim, Y. Estrin, B.C. De Cooman, 2009, Strain rate sensitivity of C-alloyed, High-Mn, TWIP steel, Steel Research International, 80(7), 493-498.

DEFENCE SCIENCE AND TECHNOLOGY ORGANISATION
DOCUMENT CONTROL DATA

1. PRIVACY MARKING/CAVEAT (OF DOCUMENT)

2. TITLE

Effects of Dynamic Impact Loading on Microstructure of FCC (TWIP) Steel

3. SECURITY CLASSIFICATION (FOR UNCLASSIFIED REPORTS THAT ARE LIMITED RELEASE USE (L) NEXT TO DOCUMENT CLASSIFICATION)

Document	(U)
Title	(U)
Abstract	(U)

4. AUTHOR(S)

C.H. Choi, C.T. Peng, B.F. Dixon

5. CORPORATE AUTHOR

DSTO Defence Science and Technology Organisation
506 Lorimer St
Fishermans Bend Victoria 3207 Australia

6a. DSTO NUMBER	6b. AR NUMBER	6c. TYPE OF REPORT	7. DOCUMENT DATE
DSTO-TR-3004	AR-016-045	Technical Report	August 2014

8. FILE NUMBER	9. TASK NUMBER	10. TASK SPONSOR	11. NO. OF PAGES	12. NO. OF REFERENCES
	ARM 07/132		12	13

13. DSTO Publications Repository

http://dspace.dsto.defence.gov.au/dspace/

14. RELEASE AUTHORITY

Chief, Land Division

15. SECONDARY RELEASE STATEMENT OF THIS DOCUMENT

Approved for public release

OVERSEAS ENQUIRIES OUTSIDE STATED LIMITATIONS SHOULD BE REFERRED THROUGH DOCUMENT EXCHANGE, PO BOX 1500, EDINBURGH, SA 5111

16. DELIBERATE ANNOUNCEMENT

No Limitations

17. CITATION IN OTHER DOCUMENTS Yes

18. DSTO RESEARCH LIBRARY THESAURUS

Hardness, Impact strength, Microstructures

19. ABSTRACT

Armoured vehicles are primarily designed to provide protection against blast and ballistic events, however there is pressure to reduce the weight of vehicles in order to achieve improvements in range and maneouvrability combined with reductions in operating cost. To obtain improved performance without compromising blast and ballistic properties, a range of tougher, lighter and harder materials have been investigated. This work looks at the possible use of ultra-fine grain (UFG) materials to achieve the desired properties. From a fundamental viewpoint, as indicated by the Hall-Petch equation, UFG is an ideal means for hardening and strengthening a metal without changing its chemical composition and without compromising ductility.

The work described here is a microstructural investigation of TWIP steel that has been subjected to blast loading. It is found that the pre-blast technique reduced the grain size of the TWIP steel significantly and that the dominant deformation mechanism of the grain refined material was dislocation slips. The reduction in grain size resulted in a considerable increase in material hardness.